Wavelength-dependent resolution and electron energy distribution measurements of image intensifiers

Robert Brooks, Martin Ingle, James Milnes and Jon Howorth
Photek Ltd. 26 Castleham Road, St. Leonards-on-Sea, East Sussex, TN38 9NS, UK
John Hutchings
Herzberg Institute of Astrophysics, National Research Council of Canada

ABSTRACT

Electrons generated in photocathodes have a range of energies and may exit the outer layer of the photocathode with a certain distribution (possibly isotropic). In a proximity-focussed image intensifier where there is a strong electric field between the photocathode and the micro-channel plate (MCP) electrons ejected at an angle will follow a trajectory defined by the exit velocity of the electron and the strength of the field. A small spot of light projected onto the photocathode will result in a point spread function determined by the size of the gap, the field applied across it and the magnitude of the radial energy component of the electrons. By using photon counting and centroiding techniques, the events occurring on the screen of an image intensifier have been integrated and used to measure the diameter of the projected spot (~ 5 micron diameter) thus giving a measure of the resolution of the tube. At short (UV) wavelengths the spread of electron energies is larger and the average radial energy component is larger than at longer (visible) wavelengths. Hence the resolution is better in the visible.

Resolution measurements as a function of wavelength of solar blind and S20 intensifiers show a dip in the measured spot size and hence a localised peak in the resolution in a short range of wavelengths in the UV. Combined with data obtained from measuring the electron energy distribution that shows a narrowing of the distribution in the same region, this shows evidence of multiple photoelectrons being generated within the photocathode. Such electrons would have lower energies resulting in higher measured resolution and a narrower electron energy distribution profile.

KEYWORDS: photocathode, resolution, image intensifier, S20, solar blind, bialkali

INTRODUCTION

Photek is currently participating in a contract to build UV imaging detectors for the UVIT (Ultra-Violet Imaging Telescope) package on the Indian Space Agency's ASTROSAT space telescope mission. The UVIT detectors are photon counting camera systems, consisting of multi-channel plate image intensifiers, with a phosphor screen fibre optic output window bonded to a Fill-Factory Star250 CMOS sensor. Three detectors will be flown aboard the mission with different photocathodes to give sensitivity at deep-UV and UV wavelengths (130 to 350 nm). Three detectors will be used on the system. One has a Caesium-Iodide photocathode on a MgF_2 window to give Far-UV (FUV) sensitivity, one has a "solar-blind" telluride cathode for Near-UV (NUV) and one that operates in the visible with a low-noise S20 photocathode.

There is a requirement to be able to resolve two objects in the sky to better <1.8 arc-seconds. Taking account of the telescope optical system one arcsecond in the sky gives 25 microns across the detector. The requirement is to build detectors with resolutions better than 30 microns at wavelengths of 185nm to 400nm.

The main factors affecting the resolving power of the intensifier are

1) The distance between the photocathode and the MCP
2) The electric field applied between the photocathode and the MCP
3) The energy of photoelectrons as they exit the photocathode.

Consider a situation with monochromatic light incident on photocathode. A photon first of all needs to have an energy greater than the band gap E_g and to be absorbed by the layer. It needs to promote an electron from the valence band into the conduction band and this electron needs to make its way to the vacuum interface. Energy will be lost on the way to the surface mainly by phonon scattering from lattice interactions. In order to be released from the surface to the vacuum the electron must have sufficient energy to overcome the surface barrier, so its residual energy needs to be greater than the electron affinity E_A.

In an idealised case with no scattering the minimum energy required for a photon to produce photoemission is:

$$hv = (E_g + E_A) \qquad (1)$$

Variation in the amount of energy lost due to phonon scattering causes a spread of electron energies leaving the photocathode. Electrons generated in the layer do not necessarily travel in the same direction as the initial photon, in fact there is no reason to consider why they should not be released isotropically. Since the scattering length of electrons within the thin layer is very short, maybe a few atomic layers, it is safe to say that the point of electron release from the photocathode surface is close to the point at which the photon was absorbed. The result is that a beam of photons tightly focussed to a tiny point on the photocathode should generate the release of electrons from the surface from a point of similar size. The electrons will exit the photocathode into the vacuum with a spread of velocities in terms of both magnitude and direction.

With a large gap between the photocathode and the MCP and zero applied field, the electrons will drift across to the microchannel plate where they will impact on the NiCr coated microchannel plate. The spread of the electrons will result in a huge "footprint" of electrons on the MCP, however the MCP has a work function that the electrons won't be able to overcome without some excess energy.

By applying a strong electric field ~ 1000 Vmm^{-1}, the electrons will be deflected such that even those that exit the photocathode at shallow angles to the surface will be drawn across to form a much tighter footprint although one that is still significantly larger than that the initial light spot. Smaller gaps and stronger electric fields should help reduce the size of the footprint and the energy distribution is also affected by energy of the photons. More energetic photons will result in more energetic photoelectrons, hence the spread across the MCP will be greater. The shorter the wavelength of the light, the more energetic the photons and hence the larger the footprint.

More spreading will occur between the channel plates and the screen to create a large charge footprint at the phosphor screen. With a camera imaging the events on the screen and by running photon counting software with a centroiding algorithm an image with sub-pixel resolution can be obtained. Centre of gravity detection algorithms in software allow the spatial position of the event to be referenced back to the impact point on the front of the first microchannel plate. Measurements of the diameter of the spot in the image then enable us to measure the resolution of the detector. Some authors [2,3] have described theoretically the spreading of electrons released from photocathodes and one [4] has produced a diagram showing the effect of cathode to channel plate gap size and applied electric field on the resolution of a typical proximity focussed image intensifier.

EXPERIMENTAL

A light source consisting of a collimated white light (tungsten) or UV (deuterium lamp) is incident onto the entrance slit of a Czerny-Turner type F/4.2 Specs monochromator (figure 1). Varying the lamp current for the white light or slit width for the UV lamp controls light intensity. The selected wavelength of light from the monochromator passes through a 10 micron diameter pinhole (laser cut into a thin stainless steel disc) mounted at the exit slit position. The light passes through a short tube into the dark box and using a lens doublet is demagnified and brought to focus at the front end of the tube. The lens doublet consists of two plano-convex lenses, positioned with convex sides facing together. The fused silica lenses have 150mm focal length and are 12.7 mm in diameter. Focussing is achieved by moving the lens doublet on a motorised linear positioning stage with external controls that can be operated from outside the dark box. A digital vernier with external readout gives the position of the lens to enable focus points to be found more quickly. All the equipment described is mounted on an optical table to give good stability. The tube and camera are both mounted on an optical rail.

Although the flight model UVIT detectors use the fibre coupled Star 250 camera, for experimental purposes a Basler CCD camera was lens coupled to the fibre optic taper behind the screen of the image intensifiers.
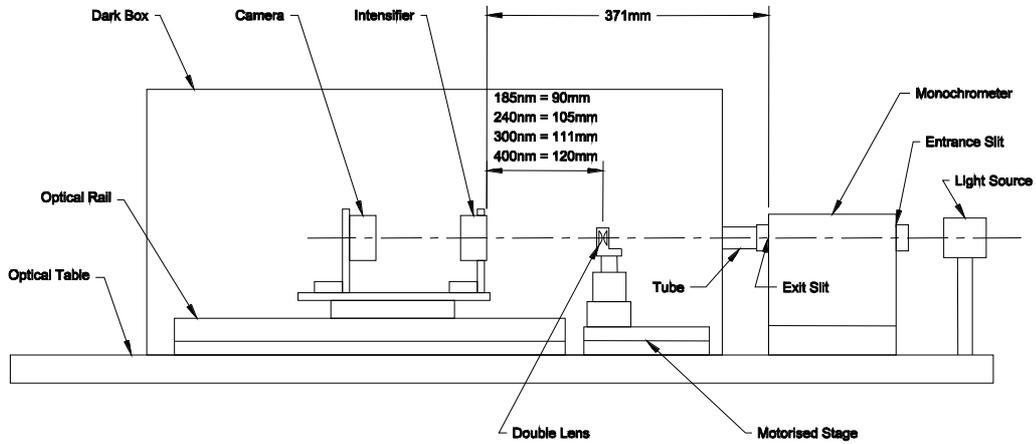
Figure (1) Diagram of resolution measurement equipment

The Photek IFS32 software allowed control of the camera its centroiding algorithm splitting each pixel into 32 bins enabled integration of an image over about half an hour with good enough statistics to measure the peak and FWHM values of the spot. From the number of pixels measured, the resolution of the tube R_d at the wavelength λ in dimensions of length (ie microns) can then be found by:

$$R_d(\lambda) = \frac{R_p(\lambda)d}{Nb} \qquad (2)$$

Where $R_p(\lambda)$ is the resolution in pixels at wavelength λ
d is the diameter of the tube
N is the number of pixels across the tube
b is the centroid binning factor

The normal method of quantifying the spread of the photon counts is Full Width at Half Maximum (FWHM), where a line is drawn through the peak in the middle and graphed as shown in the figure below. A horizontal line was drawn

through the pixel with the most counts (6599), five columns in from the left and six rows up from the bottom. The problem with this method is ensuring that the line is drawn through the centre of the image and also most of the information contained in the pixels of the spot are thrown away as only those lying on the line contribute to the line profile. This means the line profile method is not a very accurate way of measuring the FWHM.
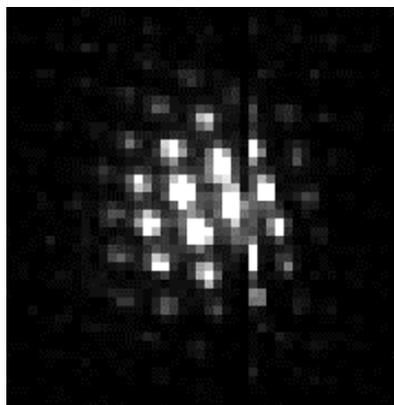
Figure (2) Centroided image of projected spot at x32 pixel binning. The hexagonal structure of the MCP pores can clearly be seen. In this example the pores are 12 microns in diameter and 15 microns from centre to centre.

Another issue when making measurements of tubes with high resolution is an image that looks like figure (2). The bright spots are actually the pores of the front microchannel plate. Note the hexagonal close packed structure. Although this gives a useful check on the scaling of the spot measurement, it also makes the FWHM measurement from a line profile through the centre of the image more difficult.

Our solution for interpreting these images and obtaining more accurate measurements is to use a radial line profile method. First of all it is necessary to find the x and y coordinates of the centre of the image. To find the mean x position, counts that occur in the same column are added together, then multiplied by the number of counts in each column by the column number. Adding all these values together and by dividing by the total number of counts gives the mean x position. A similar process for the vertical scale gives the mean y position. This is not necessarily the pixel with the highest number of counts.To find the FWHM, the values are taken of pixels radially from the centre, by averaging intensity values of pixels that are the same radial distance from the centre. The resulting plot of mean intensity vs radial distance allows the FWHM to be measured (figure 3).
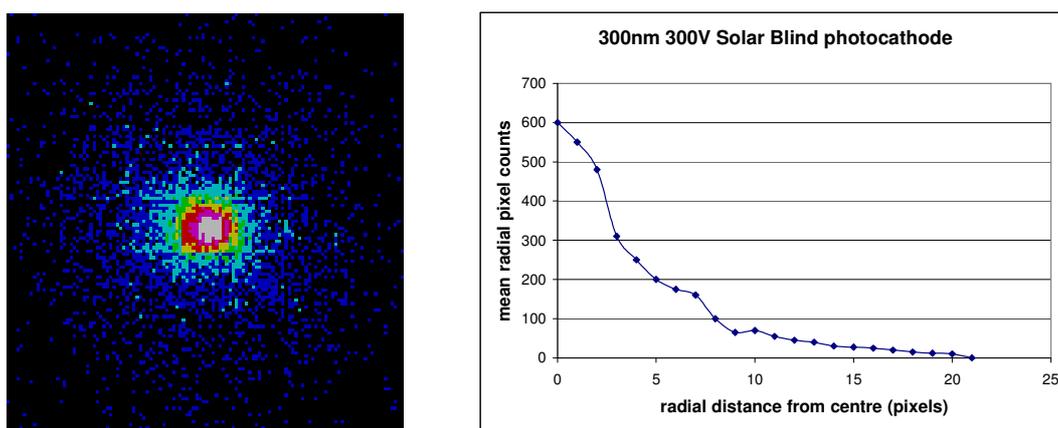
Figure (3) Centroided image of projected spot and graph showing line profile through the centre of the image

If the resolution of the detector is high enough that the MCP pores are resolved then this can still cause some difficulties in measuring the FWHM. It is then best to use a series of equal size pinholes located at the monochromator exit slit position to obtain a set of images. These can then be overlayed to average out the contributions from the MCP pores.

Rotating and summing the images is another way of smoothing out the pore sampling although such smoothing can artificially increase the measured FWHM of the images and we decided that the envelope of the signal peaks is the best representation of the spot size.

The images tend to have a halo around the main spot particularly in low resolution cases. Electrons incident on the MCP will either land in a MCP pore or on the webbing in between. Electrons landing on the webbing will either be absorbed or may bounce off the surface and get drawn back towards the MCP by the electric field. Depending on their velocity when they leave the surface they could land in a neighbouring or nearby MCP pore or even one that is some distance away. It is possible they may then bounce again if they do not enter a pore. Electrons are more likely to bounce if they impact at non-normal incidence, so the larger the front gap and the weaker the electric field, the larger the halo will be. Large halos can distort the image significantly.
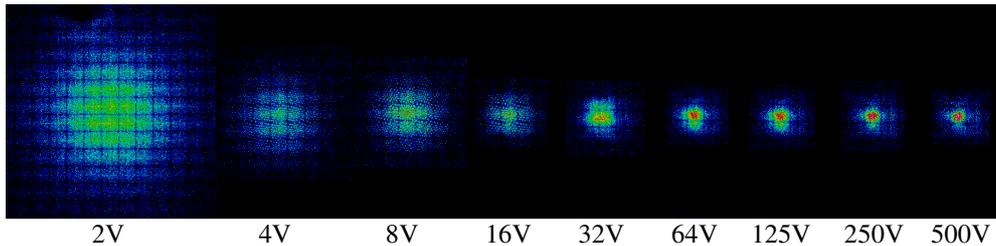
Figure (4) Solar blind image intensifier tube running at 185 nm, 0.21 mm cathode-MCP gap
(note the grid pattern superimposed on the images is an artefact of the centroiding algorithm)

Varying the cathode-MCP voltage and hence the electric field at a fixed wavelength and acquiring images for each voltage enables the effect of the electric field on resolution to be monitored (figure 4). Alternatively, the voltage can be fixed and the wavelength of light varied using the monochromator.

The point spread function of the first stage of a proximity focus tube is given by Eberhardt [1]

$$P(r) = P(0)\exp(-r^2 V / 4L^2 V_r) \qquad (3)$$

which can be solved as

$$\text{FWHM} = 3.33L(V_r / V)^{\frac{1}{2}} \qquad (4)$$

where P(0) is the peak value of the point spread function, r is the radial distance from the location of the maximum, V is the gap voltage, L is the gap length, V_r is the mean radial emission energy of the photoelectrons.

RESOLUTION MEASUREMENTS

The measurements and image analysis were carried out at Photek Ltd. Hertzberg Institute of Astrophysics also made their own analysis of the images, which show close agreement.
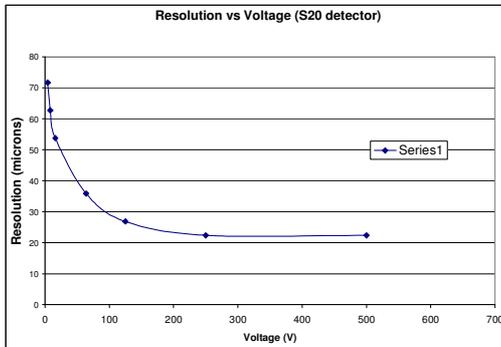
Figure 5A
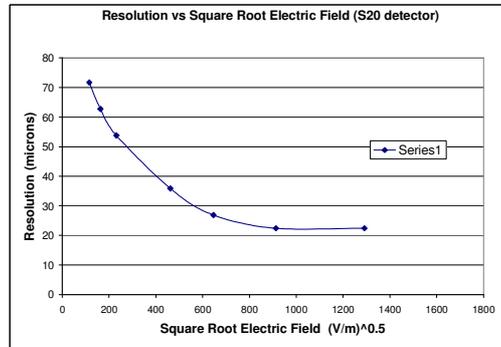
Figure 5B
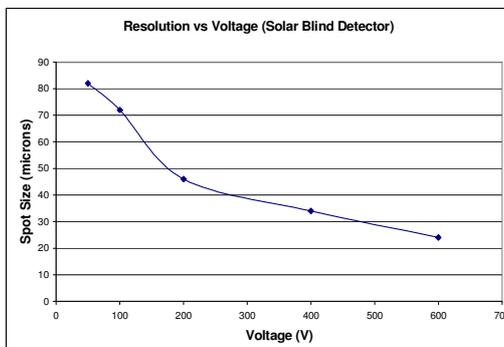
Figure 5C
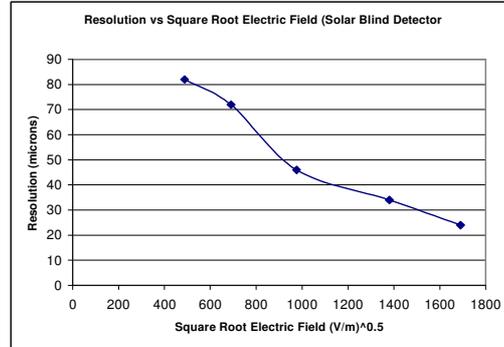
Figure 5D

Figure 5 Resolution measuements as a function of (A) Voltage – S20 detector (B) Square Root Electric Field - S20 Detector (C) Voltage – Solar Blind detector (D) Square Root Electric Field – Solar Blind Detector
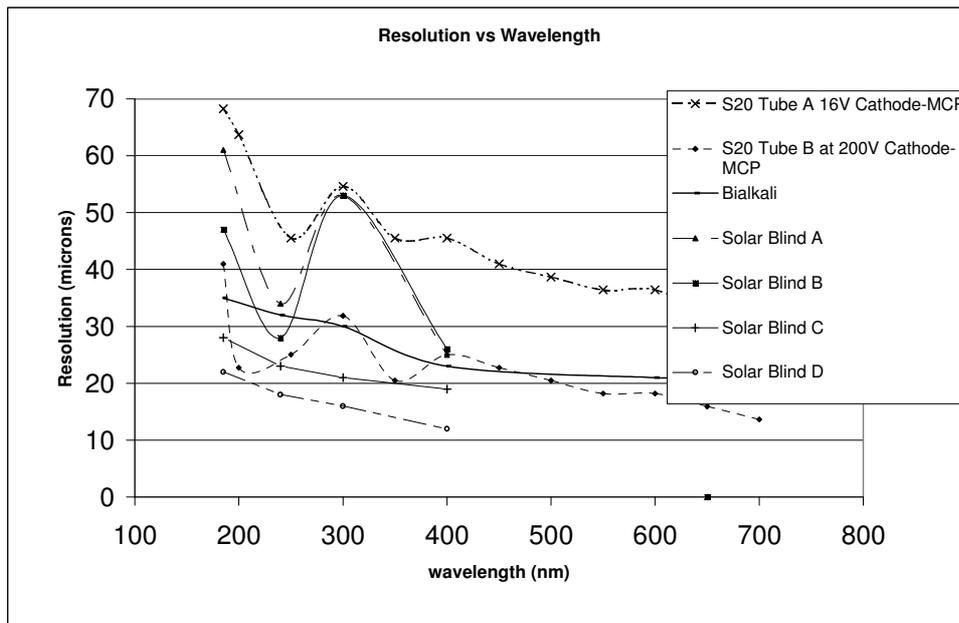
Figure 6 Resolution measurements as a function of wavelengthfor different tubes.

The graphs in figure 5 show the effect of varying the front gap voltage, plotted either as a voltage or square root of the electric field. A simplistic model of resolution as a function of square root electric field should give a straight line fit, however at there are other effects to consider. Photocathode surfaces are not perfectly smooth and there maybe micron scale distortions in the surface. Studies by [5] show that combining these distortions with electric fields in proximity tubes distorts the field near the cathode from which the electrons can gain additional transverse energy. This effect can dominate the resolution at low energies and is strongly dependent on initial electron energy. As the field increases this initial energy and the topography of the surface become less significant in comparison to the energy the electron gains from the field. In these devices the pore spacing of the microchannel plate (15 micron) will limit the ultimate resolution that can be achieved.

The effect of constant field and varying wavelength is shown (figure 6) and generally resolution decreases steadily with wavelength as would be expected as the higher energy photoelectrons impact over a larger area on the channel plate than the lower energy ones.

On some of the solar blind tubes and our S20 tube there are sharp peaks in resolution at around 250 - 300nm. This effect could be due to the effect of generating multiple electrons per photon in the photocathode. The S20 photocathode for example, has an activation energy of around 1.1eV. With increasing photon energy more electrons are excited into the conduction band with greater energies. Electrons arriving at the conduction band with sufficient energy to generate additional hole-electron pairs from inelastic collisions with the lattice might generate two low energy photoelectrons. Theoretically, an incident photon with 3.3eV might even kick out 3 photoelectrons, obviously though with the extra energy losses in the processes, the actual energies required would be expected to be significantly higher.
These electrons will have much less energy than a single UV photoelectron and will therefore impact over a tighter area, hence giving an improvement in resolution. This could explain the peak dip at 240 nm. 300nm is probably beyond the threshold for the effect to start and at 185 nm the effect of decreasing wavelength is dominant.
This process have been seen recently by [6] and who have made seen evidence of this effect in pulse height distribution measurements of photo-multiplier tubes with S20 photocathodes. The effect was only seen by [6] in some tubes. At 565nm the photon energy is 2.2 eV, which is twice the activation energy and would be the minimum possible threshold for two electrons to be released, however [6] saw no evidence that this was enough and believe the effect started below 340nm (3.7 eV), peaked at 280 nm (4.4eV) and ended above 250nm (5eV).

Various possibilities exist for electron excitation and their motion to the cathode surface and across the vacuum gap to the MCP.

1) A single electron is generated and proceeds to leave MCP
2) A single electron is generated and is absorbed by the photocathode
3) Two lower electrons are generated and both follow the same trajectory to the MCP
4) Two lower electrons are generated and follow different paths to the MCP
5) Two lower electrons a generated and one is absorbed within the photocathode (the other proceeds as 3 or 4)
6) Two lower electrons a generated and both are absorbed within the photocathode

Possibilities 2 and 5 clearly do not matter as neither will result in a detected photon. 3 and 5 will result in better resolution than the conventional case 1. 4 will produce a little improvement depending on the trajectories of the electrons.

Other tubes including solar blinds C and D (UVIT prototype detectors) and a bialkali tube do not feature this resolution dip. This is difficult to explain why this would be the case, but we do know that [6] only see the effect on pulse height distribution. The photocathode process is slightly different between detectors A and B and detectors C and D detectors and/or the activation energy is different. Since the bialkali photocathode does not have a Cs surface layer to lower its workfunction unlike the S20, it has a higher activation energy than the S20. Further studies by [6] of numerous photomultipliers have shown there is considerable variation in activation energy between S20 tubes.

ELECTRON ENERGY DISTRIBUTION MEASUREMENTS

A study by [7] investigated the electron energy distributions of S20 photodiodes and saw a broadening of the mean photo-electron energy with decreasing wavelength from around 300 nm to around 270 nm. Below 270 nm a similar narrowing effect was seen. They combined this with photometry data that showed maxima and minima occurring in the UV at integral multiples of constant photon energy. The maxima correspond to energy thresholds where there is sufficient energy to release 2 or 3 or 4 etc. low energy electrons per incident high energy photon. The authors imply these effects are not seen in all the tubes they measure.

We have made our own retarding potential measurements of a solar-blind tube, operated in diode mode by negatively biasing the photocathode and using the front MCP as an anode to collect photocurrent measured with a pico-ammeter. A deuterium lamp and monochromator were used to illuminate the photocathode and at wavelengths between 214 nm and 350 nm. The bias voltage was adjusted gradually from a reversed biased state (with zero photocurrent) to a forward biased state and the photocurrent recorded at each voltage interval. The absolute value of the photocurrent drops as would be expected with increasing wavelength due to the decrease in sensitivity of the photocathode, in addition to other factors such as lamp output. The drop from 300 nm to 350 nm is most dramatic, as this is a solar-blind photocathode with a sharp drop in sensitivity in this region.

The interesting information is found by examining the voltage range over which the device switches on. Taking the derivative $\frac{dI}{dV}$ of the data, plotting this also against applied voltage and measuring the FWHM (in Volts) of the derivative gives a measure of the distribution of the electron energies (in electron-volts) as they are released from the photocathode. The smaller the value, the tighter the spread of electron energies. See figure 7
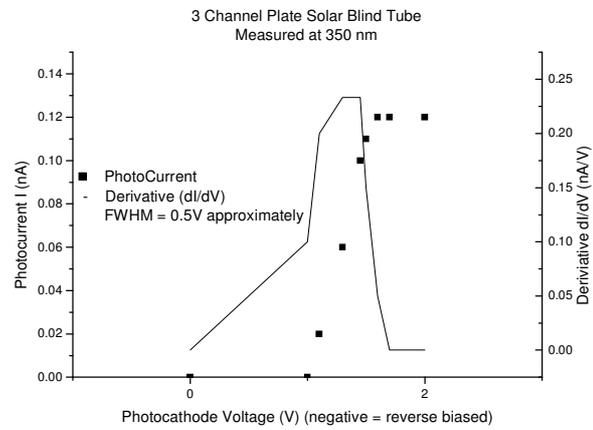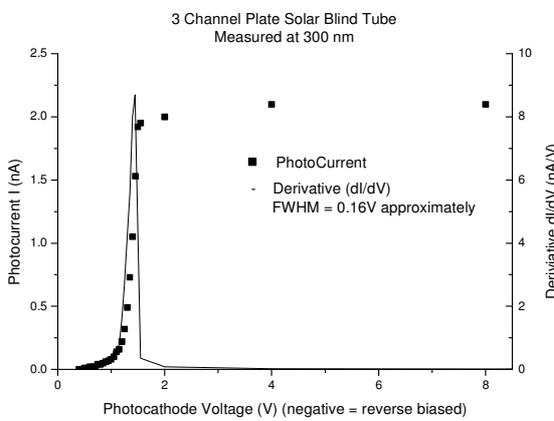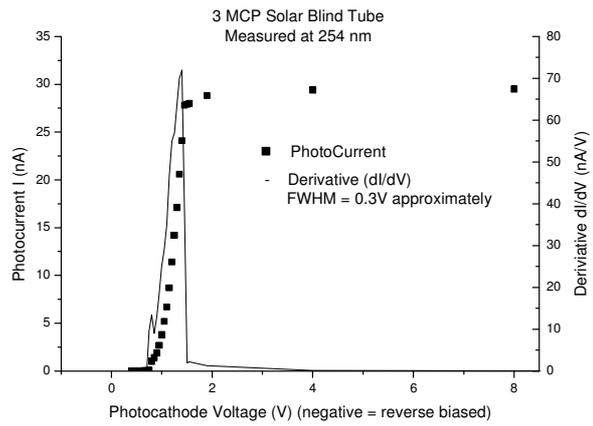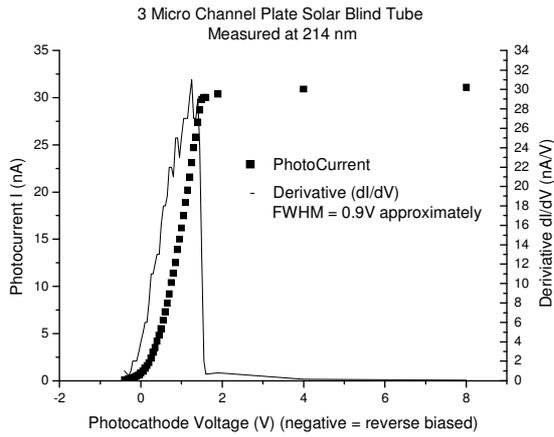
Figure 7: Electron Energy Distribution plots and $\dfrac{dI}{dV}$ plots for 3 MCP Solar Blind Tube at different wavelengths

The spread of electron energies at a given wavelength should directly affect the resolution of the detector. The tighter the spread, the higher the measured resolution should be, therefore one would expect the distribution to be tighter at longer wavelengths than at short wavelengths. Figure 8 shows the measured mean photoelectron energy distribution as a function of wavelength.
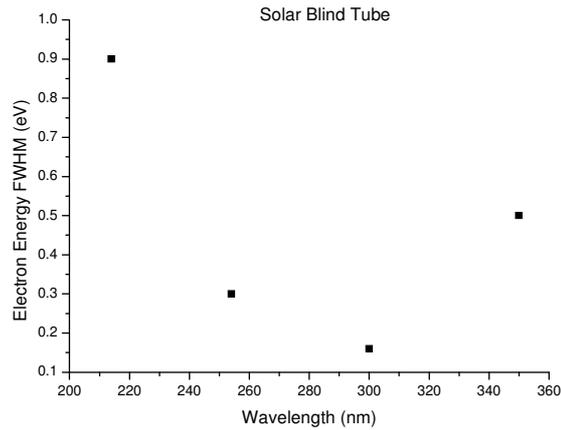
Figure 9 Electron energy FWHM plotted as a function of wavelength – Solar Blind Tube

The distribution is tighter between 215 and 350 nm as one would expect, but there is a sharp dip in between. The position of the valley in the graph lies between 260 and 300 nm. This is at a slightly longer wavelength than dip seen in the resolution spot size data.

CONCLUSIONS

Measurements have been made of the resolution of image intensifier tubes. The data shows in some cases there are peaks in resolution performance in the UV. There is some correlation between these results and those obtained from electron energy distribution measurements on a solar blind image intensifier tube where a dip is evident in a plot of energy spread vs. wavelength in a similar region of the UV to that where the dip is seen. A possible explanation for these anomalies is that excitation process within the photocathode may generate two low energy, rather than one high energy, electrons and if one or both of these electrons reach the vacuum level of the photocathode, they will lower the average radial spread of electrons reaching the anode and also reduce the FWHM of the electron energy distribution. This hypothesis is supported by data acquired by [6] who have detected these lower energy electrons in the UV in pulse height distribution measurements of some S20 photomultiplier tubes.

REFERENCES

1) Eberhardt EH, "Image transfer properties of proximity focused image tubes" *Appl. Opt.* **16** No. 8 2127-2133 1977
2) Bradley DJ, Allenson MB, Holeman BR , "The transverse energy of electrons emitted from GaAs photocathodes"*J. Phys D: Appl. Phys.*, **10**, 1977
3) Martinelli RU, Fisher DG, "The application of semiconductors with negative electron affinity surfaces to electron emission devices", *Proc.IEEE*, **62**, No. 10, 1974
4) Lyons A, "Design of proximity-focused electron lenses" *J. Phys. E: Sci. Instum.*, 18, 1985
5) Martinelli RU*, "Effects of cathode bumpiness on the spatial resolution of proximity focused image tubes" *Appl. Opt.* **12** 1841-5, 1973
6) Downey R J, D.Phil Thesis, University of Sussex, UK, (2006)
7) Johnson CB, Bonney L, Floryan RF, "Some ultraviolet spectral sensitivity characteristics of broadband multialkali photocathodes" SPIE **932** *Ultraviolet Technology II*, 285-290 (1988)